# Proceedings of the Seventh World Conference on Earthquake Engineering

VOLUME 1

Geoscience Aspects

Part 1

September 8-13, 1980

# PROCEEDINGS OF THE SEVENTH WORLD CONFERENCE ON EARTHQUAKE ENGINEERING

September 8-13, 1980
Istanbul, Turkey

VOLUME

1

# GEOSCIENCE ASPECTS, PART I

**SEISMIC WAVE PROPAGATION**

**SEISMIC SOURCE STUDIES**

**SEISMIC MICRO- AND MACRO- REGIONALIZATION**

**SEISMIC RISK ANALYSIS**

TABLE OF CONTENTS

A STOCHASTIC SOURCE MODEL FOR SYNTHETIC STRONG-MOTION SEISMOGRAMS ..... 1
William B. Joyner, David M, Boore

ON THE RATHER LONG-PERIOD EARTHQUAKE GROUND MOTIONS DUE TO DEEP GROUND STRUCTURES OF TOKYO AREA ..... 9
Kazuoh Seo, Hiroyoshi Kobayashi

PREDICTION OF INDUCED SEISMIC PHENOMENA RELATED TO RESERVOIRS ..... 17
Thomas Vladut

A GALERKIN FINITE ELEMENT MODEL FOR TSUNAMI RUN-UP ..... 25
T.C. Gopalakrishnan, C.C. Tung

GROUND MOTION ON RIDGES UNDER INCIDENT SH WAVES ..... 33
Francisco J. Sanchez-Sesma, Jorge A. Esquivel

SIMULATION OF TRAVELLING SEISMIC WAVES FOR LIFELINE ENGINEERING ..... 41
S. Takada, J.P. Wright, H. Ohiro

SHORT-PERIOD SEISMIC RADIATION AND ESTIMATION OF STRONG MOTION FROM LARGE EARTHQUAKE ..... 49
A.A. Gusev, S.A. Fedotov

SOME EFFECTS OF ANISOTROPY ON THE WAVE PROPAGATION IN SATURATED POROUS MEDIA ..... 57
Hans Van der Kogel, Joel Sweet

DISSIPATION AND DISPERSION OF SEISMIC WAVES IN WATER-SATURATED STRATA ..... 65
Men Fulu

QUANTITATIVELY-BASED SOLUTIONS OF SOME PROBLEMS OF ENGINEERING SEISMOLOGY ..... 73
A.G. Nazarov, S S. Darbinian, R.O. Amasian, N.K. Karapetian, S.A. Pirusian, L.A. Mkhitarian

GROUND MOTION NEAR A STRIKE-SLIP VERTICAL DISLOCATION IN MULTI-LAYERED ELASTIC MEDIUM ..... 81
M. Dravinski

INTERRELATIONS OF FAULT MECHANISMS, PHASE INCLINATIONS AND NONSTATIONARITIES OF SEISMIC WAVES ..... 89
Masanori Izumi, Takahide Watanabe, Hiroshi Katukura

SEISMOTECTONIC IN EARTHQUAKE ENGINEERING ..... 97
Milan Arsovski

AN AFTERSHOCK MECHANISM ORIGINATED FROM FLUID FLOW ..... 102
Ching-Shi Liu, David T.Tang, Nien-Tsu Tseng

CORRELATION BETWEEN SEISMIC VIBRATION PARAMETERS AND TYPE OF FAULTING ..... 107
Aptikaev, F., Kopnichev, J.

WAVE PROPAGATION PROPERTIES OF A MULTI-PILE REINFORCED SOIL LAYER BY A CONTINUUM MIXTURE THEORY ..... 111
Yutaka Togashi, Masanori Iiba

ACTIVE FAULTS, PALEOSEISMOLOGY, AND EARTHQUAKE HAZARDS ..... 115
Robert E. Wallace

THE GEOLOGICAL CONDITIONS OF SEISMICITY OF THE SOUTHERN SLOPE OF THE GREAT CAUCASUS ..... 123
B.A. Borissoff

OBSERVATION AND ANALYSIS OF MICROTREMORS UNDERGROUND ..... 131
Teiji Tanaka, Kaio Osada

OBSERVATION OF LONG-PERIOD MICROTREMORS WITH SPECIAL REFERENCE TO AN EVALUATION OF LONG-PERIOD SEISMIC MOTIONS ON THE EXTREMELY DEEP SOIL DEPOSIT ..... 139
Hiroshi Kagami, C. Martin Duke, George Liang, Jun Horita

MICROZONATION OF SLOPES IN A SEISMICALLY ACTIVE FOOTHILL REGION-A CASE STUDY ..... 147
Bing C. Yen, Roberto Condoretti

AN ATTEMPT OF MICROZONATION IN AND AROUND SENDAI CITY ..... 155
Yoshihiro Sugimura

APPLICATION OF SHEAR WAVE VELOCITY ON SEISMIC MICRO-ZONING ..... 163
Shou Peixiu, Liu Zengwu, Xu Yiaotin

SEISMOTECTONIC ZONING OF TURKEY USING THEORETICAL MECHANICS ..... 169
David Cummings, David J. Leeds

MICROEARTHQUAKE STUDIES AND SEISMICITY OF AKKUYU (TURKEY) NUCLEAR POWER PLANT SITE ..... 177
K. Ergin, S. Büyükaşıkoğlu

SEISMIC ZONING AND OTHER SEISMIC PARAMETERS CONSIDERATION FOR IRAQ ..... 185
Sahil A. Alsinawi, Haqi I. Moosawi

REGIONAL VARIATIONS IN THE RUPTURE LENGTH-MAGNITUDE RELATIONSHIPS ..... 193
Hemendra K. Acharya

SEISMICITY SURVEY OF TEHRI DAM REGION PRIOR TO THE RESERVOIR IMPOUNDING ..... 197
Ashwani Kumar, P.N. Agraval, Viera Masih

DISCUSSION ON TILT DATA FOR TWO INDIAN SITES ..... 201
S.K. Mam, P.N. Agrawal

ON THE DEEP UNDERGROUND STRUCTURE OF TOKYO METROPOLITAN AREA ..... 205
Etsuzo Shima

EURASIAN-AFRICAN PLATE BOUNDARY IN SOUTHERN TURKEY AND EASTERN MEDITERRANEAN ..... 209
Silva Büyükaşıkoğlu

SEISMIC ACTIVITY IN THE GERMAN DEMOCRATIC REPUBLIC ..... 213
W. Sponheuer, G. Grünthal, A.Kunze, P.Bormann

STUDY OF REGIONAL CHARACTERISTICS OF EARTHQUAKE MOTIONS BASED ON ACTIVITY IN JAPAN ..... 217
Masakazu Ozaki

COMPREHENSIVE STUDY OF SEISMICITY AND ASSOCIATED PHENOMENA IN THE KOYNA REGION (INDIA) ..... 221
J.G.Padale, P.D.Gosavi, S.C. Marvadi, S.K. Guha

BASIC REQUIREMENTS FOR MICROZONATION ..... 225
Mehmet A. Sherif, Isao Ishibashi

MICROSEISMS OF THE NOHBI PLAIN IN JAPAN ..... 229
Naotzune Taga, Tadashi Miyazaki

EXPECTED MAXIMUM MAGNITUDE, INTENSITY AND PEAK HORIZONTAL GROUND ACCELERATION MAPS OF THE HIMALAYAN REGION ..... 233
K.L. Kaila, N. Madhava Rao

A METHOD FOR PRESUMING DEEP GROUND SOIL STRUCTURES BY MEANS OF LONGER PERIOD MICROTREMORS ..... 237
Kikuji Kobayashi

A MICROSEISMIC STUDY IN THE DERBENDIKHAN DAM AREA NORTH EASTERN IRAQ ..... 241
Sahil A. Alsınawi, Basil S. Ayar

A WORLD MAP OF SEISMIC RISK AND ITS APPLICATION TO INSURANCE ..... 245
G. Berz, A. Smolka

SEISMOTECTONIC IMPLICATIONS OF RELATIVE MOTIONS BETWEEN THE AFRICAN ARABIAN AND TURKISH PLATES ..... 253
W. Harsch, T. Kuepfer

ON THE SYSTEMATICS IN DEFINING SEISMIC ZONES ..... 261
B. Rast, R. Saegesser

SEISMIC HAZARD ANALYSIS FOR ZONES OF INTERMEDIATE SEISMICITY ..... 269
Carlos S. Oliveira

CONSISTENCY OF PROBABILISTIC SEISMIC RISK METHODS ..... 277
John G. Anderson

SEISMIC RISK MAPS IN TURKEY, IRAN AND MEDITERRANEAN AREAS ..... 285
Sadaiku Hattori

试读结束，需要全本PDF请购买 www.ertongbook.com

AN INVESTIGATION ON THE INFLUENCE OF LARGE MAGNITUDE EARTHQUAKES ON SEISMIC RISK ..... 293
Ricardo T. Duarte

UNCERTAINTY ANALYSIS IN THE EVALUATION OF SEISMIC RISK ..... 301
M. Semih Yücemen

A PRELIMINARY ASSESSMENT OF SEISMIC HAZARD FOR TURKEY ..... 309
Rıfat Yarar, Oktay Ergünay, Mustafa Erdik, Polat Gülkan

THE USE OF EXPERT OPINION IN THE ESTIMATION OF EASTERN UNITED STATES EARTHQUAKE HAZARD ..... 317
Christian P. Mortgat, Kenneth W. Campbell, Lawrence H. Wight

AN ENGINEERING ANALYSIS OF THE SEISMIC HISTORY OF NEW YORK STATE ..... 324
Dimitri Athanasiou-Grivas, Rune Dyvik, Jonathan Howland

DISTRIBUTION OF STRUCTURE'S-PERIOD-DEPENDENT SEISMIC RISK IN JAPAN ..... 331
Tsuneo Katayama

SEISMIC RISK ESTIMATES FOR CENTRAL EUROPEAN SITES ..... 339
V. Karnik, Z. Schenkova, V. Schenk

NONSTATIONARY ESTIMATES OF SEISMIC HAZARD USING THE CHINESE EARTHQUAKE CATALOG ..... 347
Robin K. McGuire, Theodore P. Barnhard

A HOMOGENEOUS ALTERNATING MARKOV MODEL FOR EARTHQUAKE OCCURRENCES ..... 355
Anne S. Kiremidjian, Thalia Anagnos

RISK ASSESSMENT OF RUNNING VEHICLES AGAINST RANDOMLY OCCURING STRUCTURAL FAILURES DURING EARTHQUAKES ..... 363
H. Kameda, H.Goto, Y. Ishikawa

ON THE PARTITIONING OF ENERGY IN LOWE DIFFRACTION PROBLEMS IN LATERALLY DISCONTINUOUS STRUCTURES ..... 371
M.H.Kazi, A. Niazy

EARTHQUAKE FORCE PREDICTION CONSIDERING LOCAL SEISMIC SOURCE ACTIVITY ..... 379
Teruo Kamada

SEISMIC RISK MAPS IN ASIAN COUNTRIES-CHINA, PHILIPPINES, INDONESIA AND OTHERS ..... 383
Sadaiku Hattori

SEISMIC RISK EVALUATION STUDIES FOR ZONES WITH SCARCE AMOUNT OF DATA ..... 387
E. Gajardo, M. Contreras

SEISMIC AND TSUNAMIC RISK IN THE PHILIPPINES ..... 391
Hemendra K. Acharya

# A STOCHASTIC SOURCE MODEL FOR SYNTHETIC STRONG-MOTION SEISMOGRAMS

William B. Joyner[1]
David M. Boore[1]

## SUMMARY

Random processes are commonly used to generate synthetic accelerograms but generally without reference to a physical model. We propose here a stochastic source model whose parameters have physical meaning. The approach is illustrated by calculation of synthetic accelerograms for the 1966 Parkfield, California earthquake at the Temblor recording site.

## INTRODUCTION

We present here a method for generating synthetic strong-motion seismograms for use as input in the dynamic analysis of structures or for the determination of response spectra or other ground-motion parameters. An important basis of the method is the concept that random variability is characteristic of earthquake source processes and must be incorporated into the source model for a realistic representation of the high-frequency end of the ground-motion spectrum.

Housner (1955) was an early proponent of stochastic models of the earthquake source. Haskell (1966) and Aki (1967) used the concept in analyzing earthquake spectra, and Hanks (1979) has consistently emphasized the role of random heterogeneities in source processes. Stochastic methods are widely used for simulating earthquake ground motion for engineering purposes, though generally without any reference to a specific source model (Bycroft, 1960; Housner and Jennings, 1964). Simulation of ground motion that has a time-varying spectrum is possible using recursive filters (Jurkevics and Ulrych, 1978). The work of Rascón and Cornell (1969) is noteworthy in that they described a method whereby synthetic accelerograms were derived from an explicit stochastic source model. Although our work is in the spirit of Rascón and Cornell, we have attempted to tie the parameters of our models more closely to the physical processes at the source. Our emphasis is on the high-frequency end of the spectrum and on sites close to the source. Butler, Kanamori and Geller (1975) have used a similar approach for computing long-period motions.

## DESCRIPTION OF THE MODEL

There are three obvious ways in which the source could show random variability: (1) the velocity of rupture propagation could vary; (2) the total dislocation could vary from point to point on the fault; and (3) the shape of the dislocation-time function could vary from point to point on the fault. In the model we present here, only the total amplitude of the dislocation varies; the rupture velocity and the shape of the dislocation-time function are constant. We are also working on other models in which all three factors vary.

[1]U.S. Geological Survey, Menlo Park, California, USA 94025

The model is illustrated in Figure 1. The rupture front sweeps across the fault surface at constant velocity $V_R$. To simplify the computations we collapse the fault into a line, so we are dealing with a point source moving along a line. A very broad class of dislocation-time functions may be used; for the example to be shown here an exponential ramp is used, as illustrated in Figure 2.

The amplitude of the dislocation-time function is composed of a mean value plus a variation about the mean. We control the spectrum of the synthetic seismogram by specifying the autocorrelation function of the variable part of the dislocation amplitude; that is our stochastic description of the source. The spectra of real accelerograms tend to be more or less flat below the frequencies where attenuation controls the slope. Such a spectrum can be achieved very simply by choosing an autocorrelation function that is a negative exponential. This function is specified by a single parameter, the coherence length, which is the distance at which the autocorrelation function is down by a factor of 1/e. In the computation of the variable part of the dislocation amplitude, Gaussian white noise is generated by the computer, using a pseudo random number generator, and then is filtered with the aid of the Fast Fourier Transform by a filter designed to produce an output with the desired autocorrelation function. Starting with different samples of white noise we produce different synthetic seismograms, which form an ensemble representing the ground motion to be expected at the site.

Four parameters of the model are to be determined by fitting real strong-motion records, the mean dislocation amplitude $\bar{D}$, the standard deviation of the dislocation amplitude $\sigma_D$, the coherence length $\ell_c$, and the rise time $\tau$ (Fig. 2). To reduce the number of degrees of freedom we impose two conditions.

$$\bar{D} = \sigma_D \qquad \text{Eq. 1}$$

$$\ell_c / V_R = \tau \qquad \text{Eq. 2}$$

The first condition is not so arbitrary as might seem at first glance. If $\bar{D}$ greatly exceeds $\sigma_D$, the model ceases to be stochastic in a meaningful sense, and, if $\sigma_D$ greatly exceeds $\bar{D}$, reversal of motion is implied over a significant portion of the length of the fault, given the Gaussian distribution of D. This leaves two free parameters $\sigma_D$ and $\tau$. Our strategy for subsequent work will be to evaluate these parameters for past earthquakes by fitting strong-motion records and use the results as a basis for selecting values for the parameters in the case of design earthquakes.

The source is placed in a homogeneous halfspace with modifications to the solution to allow for the effects of low-velocity material near the surface at the recording site and in the fault zone. Without the allowance for low velocity near the surface, the synthetic seismograms would not have realistic amplitude ratios between the horizontal and vertical components. There is substantial evidence for low P velocities in the San Andreas fault zone (Mayer-Rosa, 1973; Healy and Peake, 1975; Marks and Bufe, 1979); presumably S velocities in the fault zone are also low. In the example to be shown the recording site is at a node for SV waves, but the S amplitudes

on the radial component are nearly as large as those on the transverse component. The simplest explanation of the observed amplitude ratio is that the rays are refracted in going from the fault zone into the higher-velocity surrounding rock, and, as a result, the recording site samples a different part of the radiation pattern than it otherwise would. The velocity change required to explain the observations corresponds to a P-wave time delay across the fault zone of the order of one-tenth of the values given by Healy and Peake (1975) and Marks and Bufe (1979) for some portions of the fault; thus it is quite reasonable to expect velocity changes of the required magnitude. The refraction of the rays near the surface and in the fault zone is calculated from Snell's law; the change in amplitude is calculated on the assumption that the energy flux along a tube of rays is constant.

To compute the synthetic seismograms, the dislocations at the source are replaced by the equivalent double couples, whose radiation field is calculated by the far-field formulas of Hirasawa (1970). The free-surface interaction is accounted for by applying complex reflection coefficients in the frequency domain. The solution thus includes the direct body waves but not surface waves. This should be an adequate approximation, at least for higher frequencies at sites near the source. Anelastic attenuation is accounted for by applying the Lomnitz causal Q operator described by Savage and O'Neill (1975), and another operator is applied to simulate the effect of the recording instrument.

## EXAMPLE

To illustrate the method, we have chosen to model the Temblor strong-motion record from the Parkfield, California earthquake of 1966. This earthquake occurred on the San Andreas fault, a right-lateral strike-slip fault. The rupture propagated from the hypocenter toward the southeast for a distance that is the subject of some dispute. We adopt the interpretation of A. G. Lindh and D. M. Boore (unpublished manuscript), according to which the rupture propagated a distance of about 25 km from the hypocenter at a velocity of 2.5 km/sec. The Temblor station is 16 km southeast of the postulated end point of the rupture. Guided by the distribution of aftershocks (Eaton and others, 1970), we place the line source at a depth of 6 km and choose a fault width of 7 km. P and S velocities are assumed to be 6.0 and 3.5 km/sec, respectively, for the halfspace and 4.0 and 1.1, respectively, for the Franciscan rocks at the recording site. An S-wave Q of 100 is estimated from the spectrum of the observed strong-motion record and a P-wave Q of 220 is computed from the S-wave Q on the assumption of zero energy loss in compression. Independent estimates of Q would be desirable, but we have no other data for this area.

In fitting the observed strong-motion record we first adjust the velocities in the fault zone to fit the observed amplitude ratio between the horizontal components. A fit is obtained by reducing the velocities in the fault zone by 12 percent from the halfspace values. The coherence length $\ell_c$ is then varied to obtain the correct frequency content, and the standard deviation of the dislocation amplitude $\sigma_D$ is varied to give the correct integral square amplitude. The results, using conditions (1) and

(2), are 190 cm for $\sigma_D$ and $\bar{D}$, 0.73 km for $\ell_c$, and 0.29 sec for $\tau$.

In Figures 3, 4, and 5 synthetic accelerograms for three members of the ensemble (above) are compared with the observed record (below) for each of the three components. A similar comparison is shown in Figure 6 for the velocity on the transverse component and in Figure 7 for the Fourier spectrum of acceleration on the transverse component. Figure 8 shows the five-percent-damped, pseudovelocity response spectra for the transverse component. The plus signs represent the synthetic accelerograms and the line represents the observed record.

## DISCUSSION

Figures 3 through 8 indicate that the synthetic seismograms have an amplitude envelope and a frequency content quite similar to the observed record. The synthetic seismograms lack the low-amplitude coda of surface waves and scattered body waves that is present on the observed record, but this discrepancy is probably of limited engineering significance, at least for high-frequency structures at short distances from the source.

The value of 190 cm for the mean dislocation, which results from our requirement that the mean be equal to the standard deviation, is rather high. The corresponding seismic moment of $1.1 \times 10^{26}$ dyne-cm is more than twice as high as the value of $4.4 \times 10^{25}$ obtained by Trifunac and Udwadia (1974) from an analysis of doubly integrated strong-motion records. The latter value in turn is about three times as high as that obtained by Tsai and Aki (1969) from long-period teleseismic surface waves. We do not believe, however, that these discrepancies indicate any serious defect in the method. For one thing, our requirement that the mean and the standard deviation be equal is to some degree arbitrary. For another, the record we are fitting is close to the southeast end of the fault and is significantly affected only by the dislocation near that end. Trifunac and Udwadia (1974) obtained a dislocation of 140 cm at the southeast end for a fault width of 6 km, which would correspond to a value of 120 cm for our fault width of 7 km, a value not too different from the one we obtained. The discrepancy with the teleseismic moment (Tsai and Aki, 1969) may in part be due to the fact that the teleseismic data is affected by the whole fault, whereas our site is significantly affected only by the southeast end.

We are encouraged by the comparisons of Figures 3 through 8 that this method will prove useful in generating time histories for dynamic analysis and in estimating ground motion parameters.

## REFERENCES


Aki, K. (1967). Scaling law of seismic spectrum, J. Geophys. Res., v. 72, p. 1217-1231.

Butler, R., Kanamori, H., and Geller, R. (1975). Long-period ground motion in Los Angeles from a great earthquake on the San Andreas fault (abs.), Trans. Am. Geophys. Union, v. 56, p. 1024.

Bycroft, G. N. (1960). White noise representation of earthquake, Eng. Mech. Div., Am. Soc. Civil Engineers, v. 86, p. 1-16.
Eaton, J. P., O'Neill, M. E., and Murdock, J. N. (1970). Aftershocks of the 1966 Parkfield-Cholame, California, earthquake: a detailed study, Bull. Seism. Soc. Am., v. 60, p. 1151-1197.
Hanks, T. C. (1979). b values and $\omega^{-\gamma}$ seismic source models: implications for tectonic stress variations along active crustal fault zones and the estimation of high-frequency strong ground motion, J. Geophys. Res., v. 84, p. 2235-2242.
Haskell, N. A. (1966). Total energy and energy spectral density of elastic wave radiation from propagating faults. Part II. A statistical source model, Bull. Seism. Soc. Am., v. 56, p. 125-140.
Healy, J. H., and Peake, L. G. (1975). Seismic velocity structure along a section of the San Andreas fault near Bear Valley, California, Bull. Seism. Soc. Am., v. 65, p. 1177-1197.
Hirasawa, T. (1970). Focal mechanism determination from S wave observations of different quality, J. Phys. Earth, v. 18, p. 285-294.
Housner, G. W. (1955). Properties of strong ground motion earthquakes, Bull. Seism. Soc. Am., v. 45, p. 197-218.
Housner, G. W., and Jennings, P. C. (1964). Generation of artificial earthquakes, Eng. Mech. Div., Am. Soc. Civil Engineers, v. 90, p. 113-150.
Jurkevics, A., and Ulrych, T. J. (1978). Representing and simulating strong ground motion, Bull. Seism. Soc. Am., v. 68, p. 781-801.
Marks, S. M., and Bufe, C. G. (1979). Fault-crossing P delays, epicentral biasing, and fault behavior in central California (abs.), Tectonophys., v. 52, p. 600.
Mayer-Rosa, D. (1973). Travel-time anomalies and distribution of earthquakes along the Calaveras fault zone, California, Bull. Seism Soc. Am., v. 63, p. 713-729.
Rascon, O. A., and Cornell, C. A. (1969). A physically based model to simulate strong earthquake records on firm ground, Proceedings of the Fourth World Conference on Earthquake Engineering, Santiago, Chile, v. 1, p. A1-84 to A1-96.
Savage, J. C., and O'Neill, M. E. (1975). The relation between the Lomnitz and Futterman theories of internal friction, J. Geophys. Res., v. 80, p. 249-251.
Trifunac, M. D., and Udwadia, F. E. (1974). Parkfield, California, earthquake of June 27, 1966: a three-dimensional moving dislocation, Bull. Seism. Soc. Am., v. 64, p. 511-533.
Tsai, Y. B. and Aki, K. (1969). Simultaneous determination of the seismic moment and attenuation of seismic surface waves, Bull. Seism. Soc. Am., v. 59, p. 275-287.



试读结束，需要全本PDF请购买 www.ertongbook.com

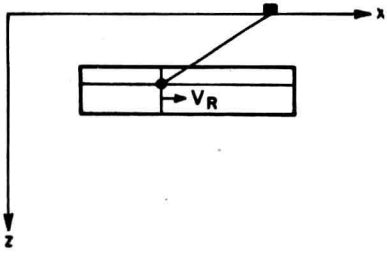


Figure 1. Diagrammatic vertical section showing the source model. $V_R$ is the rupture velocity.

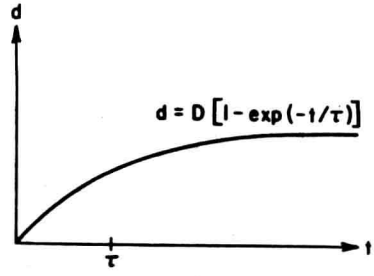


Figure 2. Dislocation d as a function of time t.

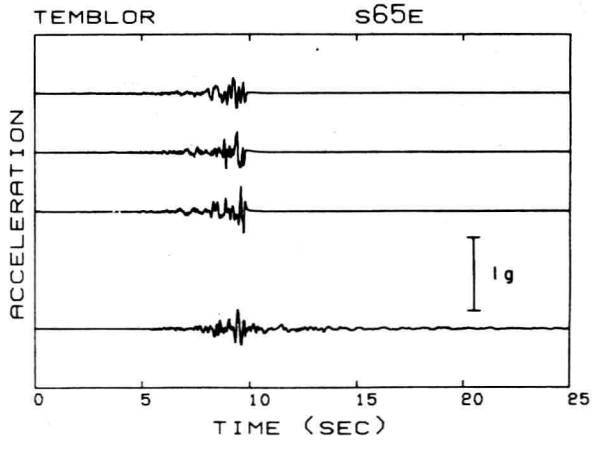


Figure 3. The radial component of acceleration. Three synthetic accelerograms above and real record below.

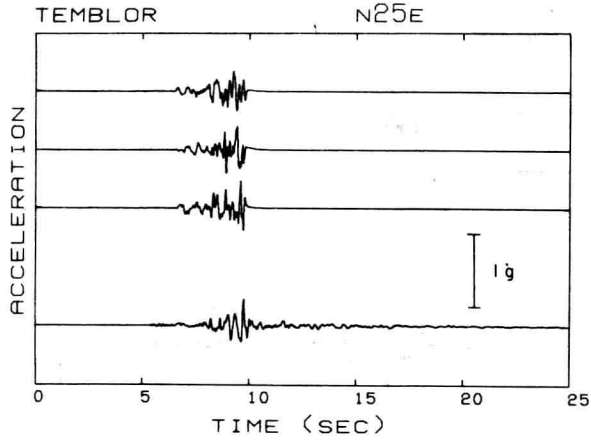


Figure 4. The transverse component of acceleration. Arrangement as in Figure 3.

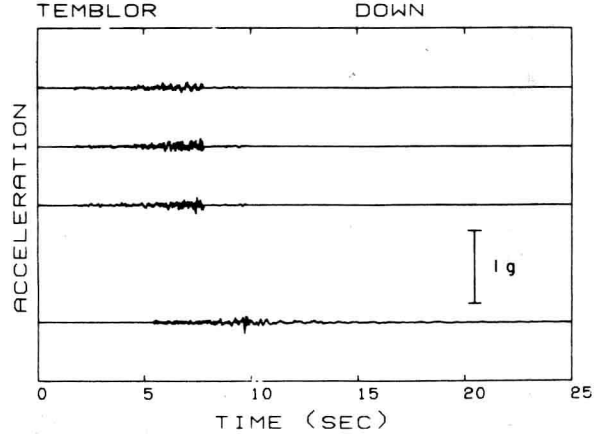


Figure 5. Vertical acceleration. Arrangement as in Figure 3.

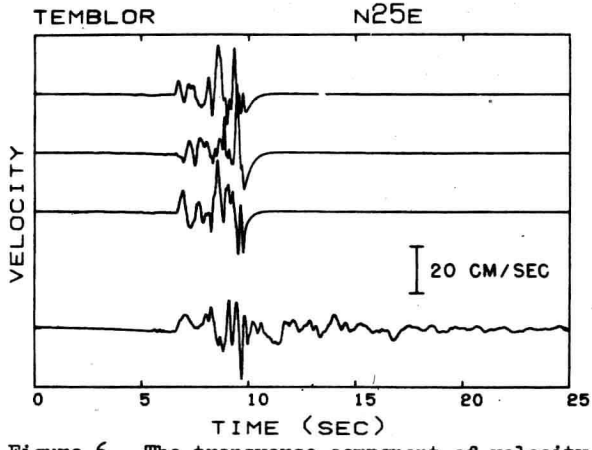


Figure 6. The transverse component of velocity. Arrangement as in Figure 3.

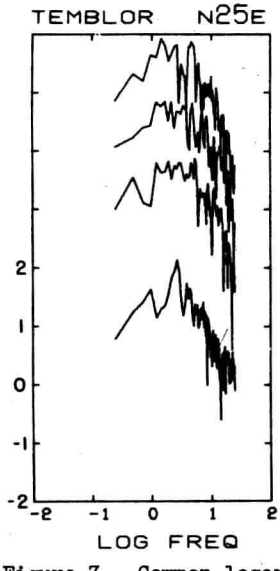


Figure 7. Common logarithm of acceleration spectra (cm/sec) for the transverse component. Spectra for the three synthetic accelerograms (above) are shifted vertically for ease of comparison; the spectrum of the real record is plotted to the scale indicated.

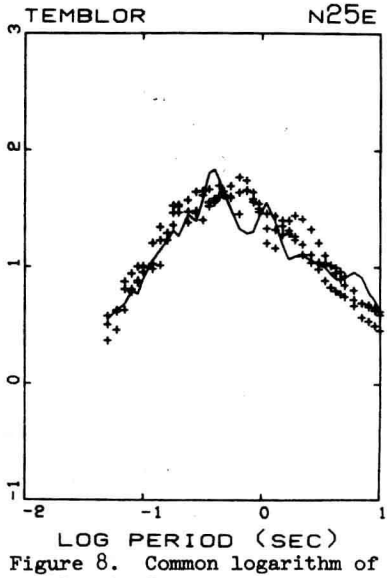


Figure 8. Common logarithm of pseudovelocity response spectra (cm/sec) for the transverse component five percent damping. Plus signs represent the synthetic accelerograms; the line represents the real record.

# ON THE RATHER LONG-PERIOD EARTHQUAKE GROUND MOTIONS DUE TO DEEP GROUND STRUCTURES OF TOKYO AREA

by

Kazuoh SEO[I] and Hiroyoshi KOBAYASHI[II]

## SUMMARY

To find characteristics of the rather long-period earthquake ground motions, array observation was performed in and around Tokyo area. During foreshocks of the Near Izu-Ohshima Earthquake of 1978, authors obtained simultaneous records, which contained rather long-period components remarkably, notwithstanding the magnitudes of these earthquakes were not so large. From studies on investigation of deep ground structure and propagation of seismic waves, it was made clear that the rather long-period components were composed of Love-waves and that they were enlarged on the halfway of propagation because of existence of thick and soft sedimentary layers of Tokyo area.

## INTRODUCTION

In the Tokyo Metropolitan Area, appearance of the rather long-period earthquake ground motions has been pointed out in case of large earthquakes, the Kanto Earthquake of 1923 for example. The rather long-period, so called in this paper, means the period range of from one to ten seconds. As interpretation of these ground motions, it has been explained that they were mainly caused by the largeness of earthquakes. But, deep subsurface ground structures on the way from seismic source to observed site should be taken into account more clearly and more minutely as one of causes to enlarge those ground motions.

Concerning these problems, array observation of earthquake ground motions, which is consisted of four stations in and around the Tokyo Metropolitan Area, is being performed. In this paper, typical records obtained by two different earthquakes will be presented to compare how these rather long-period ground motions appear. Geological condition of each station will be also checked. Distribution of deep sedimentary layers is investigated along the real wave path of the actual earthquake by means of explosion tests. And those wave paths are studied with regard to travel time, dispersion of surface wave and so on. The crustal structure and path of initial motion due to body wave had been confirmed by authors already.

By synthesizing these results, the characteristics of the rather long-period earthquake ground motions will be made more clear.

## RATHER LONG-PERIOD EARTHQUAKE GROUND MOTIONS OBSERVED IN TOKYO AREA

Array observation of earthquake ground motions is being performed at four stations using the wide-band velocity type seismometers. These stations are indicated in Fig.1, with the geological conditions(1). Among four stations, "Asakawa" is located almost directly on the firm Pre-Neogene basement, which is regarded as the seismic bedrock of Tokyo. The other sta-

[I] Assistant, [II] Professor of Earthquake Engineering, Dr.Eng.
Department of Environmental Engineering, Graduate School at Nagatsuta, Tokyo Institute of Technology, Yokohama, Japan

tions, "Ohfuna", "Ohokayama" and "Narashino", are located on deep sedimentary layers, but subsurface structures are considered to be much different each other.

Fig.2 shows two kinds of typical seismograms observed at these stations. In case of foreshocks of the Near Izu-Ohshima Earthquake of Jan.14, 1978, as shown in Fig.2.a, it can be understood that heterogeneity of individual seismograms was caused by the difference of geological conditions. For the typical example, rather long-period component which can be seen clearly at Ohokayama is not found at Asakawa entirely, while the epicentral distance is nearly the same in both cases. Epicenters of these earthquakes are plotted in Fig.1. On the other hand, in case of the Off Miyagi Earthquake of Feb.20,1978, as shown in Fig.2.b, remarkable component of rather long-period which could be seen during the Near Izu-Ohshima Earthquake does not appear. This earthquake occurred at a far distance of about 400km away from these stations, and location of epicenter is pointed in Fig.6.b.

Fig.3 shows the response spectra due to these earthquakes to compare the characteristics of ground motions between Ohokayama and Asakawa. Maximum value of velocity response is obtained by means of changing the coordinates in the horizontal plane. At the first glance, it can be known that the spectra of Ohokayama derived from two earthquakes differ considerably, while those of Asakawa are almost similar. Spectral ratio of Ohokayama against Asakawa, as shown in the lower part of Fig.3, is considered to

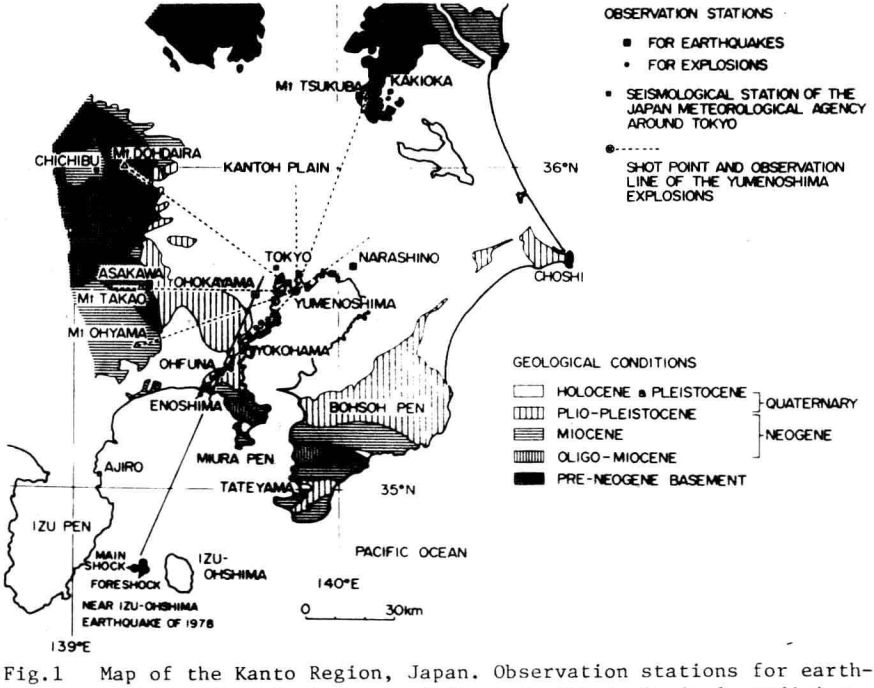


Fig.1 Map of the Kanto Region, Japan. Observation stations for earthquakes and explosions are indicated with geological conditions.

indicate the amplification of ground motions due to S-wave. Because Asakawa is the station on the seismic bedrock and similar bedrock is estimated 2.5km in depth at Ohokayama as shown in Table 1. This table was presumed based on the explosion tests(2).

At the site of Ohokayama, using the values of Table 1, the characteristics of ground motions due to SH-waves and Love-waves can be calculated theoretically as shown in Fig.4. And it is evident that the spectral ratio during the Off Miyagi Earthquake(Fig.3.b) is fitting remarkably with the amplification curve due to SH-waves(Fig.4).
In case of the Near Izu-Ohshima Earthquake, long-period component of spectral ratio in Fig.3.a is too large and the contribution due to

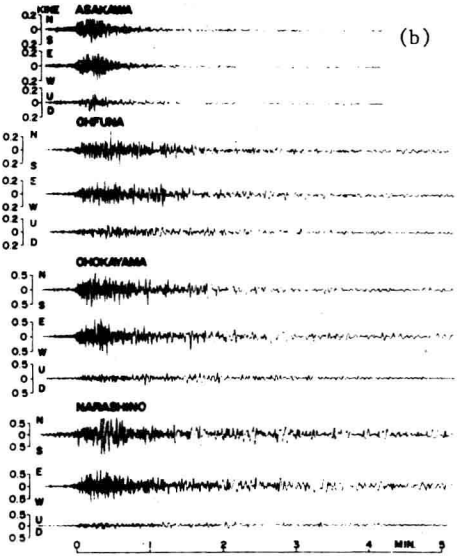


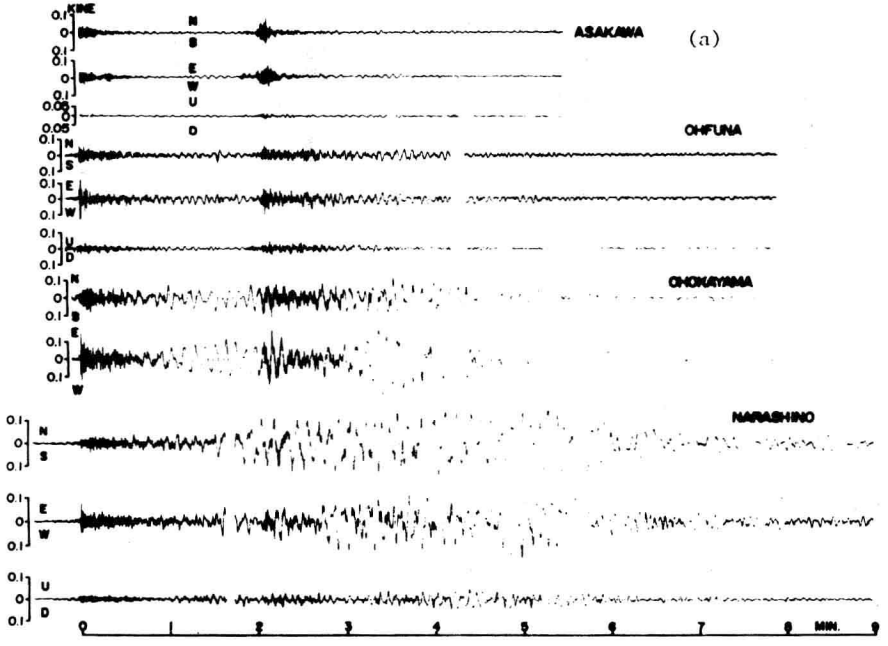


Fig.2 Seismograms obtained by array observation during the foreshocks of the Near Izu-Ohshima Earthquake of Jan.14,1978(09:45 and 09:47,M=4.9, D=0km)(a) and the Off Miyagi Earthquake of Feb.20,1978(M=6.7,D=50km)(b).



试读结束，需要全本PDF请购买 www.ertongbook.com